Research Article

Chromosomal Rearrangements in Post-Chernobyl Papillary Thyroid Carcinomas: Evaluation by Spectral Karyotyping and Automated Interphase FISH

Ludwig Hieber,[1] Reinhard Huber,[1] Verena Bauer,[1] Quirin Schäffner,[1] Herbert Braselmann,[1] Geraldine Thomas,[2] Tatjana Bogdanova,[3] and Horst Zitzelsberger[1]

[1] *Department of Radiation Cytogenetics, Helmholtz Zentrum München, German Research Center for Environmental Health, Ingolstädter Landstraße 1, 85764 Neuherberg, Germany*

[2] *Human Cancer Studies Group, Department of Surgery and Cancer, Hammersmith Hospital, G Block, Du Cane Road, London W12 0NN, UK*

[3] *Institute of Endocrinology and Metabolism, Academy of Medical Sciences of Ukraine, Vyshgorodskaya Street 69, 254114 Kiev, Ukraine*

Correspondence should be addressed to Ludwig Hieber, ludwig.hieber@helmholtz-muenchen.de

Structural genomic rearrangements are frequent findings in human cancers. Therefore, papillary thyroid carcinomas (PTCs) were investigated for chromosomal aberrations and rearrangements of the RET proto-oncogene. For this purpose, primary cultures from 23 PTC have been established and metaphase preparations were analysed by spectral karyotyping (SKY). In addition, interphase cell preparations of the same cases were investigated by fluorescence *in situ* hybridisation (FISH) for the presence of RET/PTC rearrangements using RET-specific DNA probes. SKY analysis of PTC revealed structural aberrations of chromosome 11 and several numerical aberrations with frequent loss of chromosomes 20, 21, and 22. FISH analysis for RET/PTC rearrangements showed prevalence of this rearrangement in 72% (16 out of 22) of cases. However, only subpopulations of tumour cells exhibited this rearrangement indicating genetic heterogeneity. The comparison of visual and automated scoring of FISH signals revealed concordant results in 19 out of 22 cases (87%) indicating reliable scoring results using the optimised scoring parameter for RET/PTC with the automated Metafer4 system. It can be concluded from this study that genomic rearrangements are frequent in PTC and therefore important events in thyroid carcinogenesis.

1. Introduction

The detection and quantification of tumour-specific rearrangements are important issues in cancer research and in clinical diagnosis of tumours. In particular, its significance became obvious for haematological malignancies that exhibit characteristic translocations in specific tumour subgroups [1]. Although gene rearrangements are typical for haematological malignancies, they also may occur in solid tumours as characteristic changes. This has been shown for RET/PTC rearrangements in papillary thyroid carcinoma (PTC) that fuse the RET proto-oncogene to a variety of constitutively expressed partner genes (for review see Zitzelsberger [2]). The detection of such chromosomal rearrangements was initially performed by conventional banding techniques [3]. This was further improved by the development of fluorescence *in situ* hybridization (FISH) techniques that allows a cytogenetic analysis of rearrangements on metaphase spreads as well as on interphase cell nuclei [4]. Multicolour FISH approaches such as spectral karyotyping (SKY) allowed a more detailed analysis of cytogenetic aberrations, in particular in the case of complex and hidden rearrangements [5, 6]. The analysis of interphase nuclei by FISH has the advantage that gene rearrangements can be investigated at single cell level in nonproliferating cells. An evaluation of FISH signals is usually performed by visual inspection directly from the microscopic image. In this case, cell numbers for further statistical analysis and a possible bias of the investigator

towards positivity or negativity of FISH signals indicating the rearrangement are major limitations. In order to analyse a statistically relevant number of cells, an automatic scanning system for fluorescence spot counting using a fully motorized fluorescence microscope with an eight-slide scanning stage and a high-resolution CCD camera driven by the MetaCyte software (MetaSystems, Altlussheim, Germany) has been established and optimized. To demonstrate routine application of the scanning system, the RET/PTC rearrangement in papillary thyroid carcinomas has been scored with a probe set that produces split FISH signals if a gene rearrangement is present [7]. Therefore, the parameters of the scanning system had to be optimized using cell culture models as positive and negative controls. The aims of the present study were to establish such optimised scanning parameters and to characterise chromosomal and RET/PTC rearrangements in a PTC cohort.

2. Material and Methods

2.1. Cell Cultures from PTC and Cell Lines. Primary cell cultures of 23 PTCs from children and adults from Ukraine that developed papillary thyroid carcinomas in the aftermath of the Chernobyl accident were established according to a published protocol [8]. The median age of the patients at operation was 21 years, ten patients were male, and 13 patients were female. 21 out of 23 cases were investigated for chromosomal aberrations and 22 cases for RET/PTC rearrangements. In addition, a cell line originating from a PTC (TPC1) carrying the RET/PTC1 rearrangement served as a positive control [9, 10]. As negative control we used a cell line derived from human retinal epithelium ("RPE," hTERT immortalised) that displays a normal karyotype [11]. All cell lines and primary cell cultures were grown in RPMI 1640 (PAA Laboratories, Cölbe, Germany) with the addition of Penicillin (5 IU/mL) and Streptomycin (5 μg/mL) (Gibco-BRL Life Technologies, Karlsruhe, Germany) and supplemented with 10% or 20% FBS (Sigma, Taufkirchen, Germany), respectively. Metaphase preparations from primary cultures were needed for SKY analysis. Therefore 2.5×10^5 cells were grown in 4 mL media on a sterile glass slide positioned in Quadriperm cell culture chambers (In Vitro Systems and Services GmbH, Göttingen, Germany) and addition of 0.05 μg/mL Colcemid (Roche, Penzberg, Germany) overnight arrested cells in metaphase. After 24–32 h growth, the media were removed and the slide covered with 4 mL hypotonic KCl-solution (0.075 M). After incubation under hypotonic conditions for 20 min at 37°C, 4 mL of ice-cold fixative (methanol/glacial acetic acid, 3 : 1) were added followed by another incubation step for 20 min on ice. Subsequently the solutions were removed and replaced by another 4 mL of ice-cold fixative. After 20 min incubation on ice, this last step was repeated. Finally, the slides were air-dried perpendicularly under a laminar flow. For interphase preparations, cells were directly grown on glass slides in Quadriperm cell culture chambers. Cells were fixed with Carnoy's fixative (methanol/acetic acid; 3 : 1), air-dried, and stored at room temperature for 7 days before hybridization.

2.2. SKY Analysis. Spectral karyotyping was performed as described previously in [8]. Briefly, metaphase preparations were pretreated with RNase A (0.1 mg/mL in 2 × SSC) prior to hybridization. Chromosome denaturation was achieved by treatment of the slides in 70% formamide in 2 × SSC at 72°C for 1-2 min. Subsequently the slides were dehydrated in a 70%, 90%, and 100% ethanol series and hybridized with a denatured SKY-probe mixture (SkyPaint DNA Kit, Applied Spectral Imaging, Mannheim, Germany). After hybridization (24 h), slides were washed in 0.5 × SSC for 5 min at 75°C, 4 × SSC/0.1% Tween for 2 min and H_2O_{bidest} for 2 min, both at room temperature. Probe detection was achieved using antidigoxigenin (1 : 250; Roche, Penzberg, Germany), avidin-Cy-5, and avidin-Cy-5.5 antibodies (both 1 : 100; Biomol, Hamburg, Germany) according to the manufacturers' protocols. Metaphase spreads were counterstained with 0.1% 4′,6-diamidino-2-phenylindole (DAPI) in antifade solution (VECTASHIELD mounting medium; Vector Laboratories, Burlingame, CA,USA). A minimum of 15 metaphases were analyzed to determine the karyotype of each primary culture. Chromosome aberrations were detectable by colour junctions within affected chromosomes. Image acquisition was done using a SpectraCube system, and analyses were accomplished using the SkyView imaging software (both from Applied Spectral Imaging, Mannheim, Germany).

2.3. Fluorescence In Situ Hybridization. For FISH analysis of RET/PTC rearrangements, labelling of YAC DNA probes 344H4, 214H10 and, 313F4 was carried as previously described in [7]. The YAC probes 313F4 and 214H10 map proximal to and include the RET locus, whilst clone 344H4 contains DNA sequences distal to RET. They were labelled either with digoxigenin-11-dUTP (344H4) or with biotin-16-dUTP (214H10, 313F4) using nick translation and were detected with antidigoxigenin-Cy3 antibody, followed by rat-anti-mouse Cy3 and mouse-anti-rat Cy3 for red fluorescence, and streptavidin-FITC, followed by biotin-antistreptavidin and streptavidin-FITC, respectively. A normal RET locus results into two overlapping red and green FISH signals, while split FISH signals (separated red and green signals) indicated a rearranged RET gene. Only cells with either two overlapping signals or one split and one overlapping signal were analysed to ensure completeness of the nuclei.

2.4. Evaluation of FISH Slides. For the analysis of the RET/PTC rearrangements, a fluorescence-based scanning system, Metafer4 (MetaSystems, Altlussheim, Germany), was used. This scanning system is based on a motorized Axioplan 2 microscope (Zeiss, Oberkochen, Germany), a motorized eight-slide scanning stage (Märzhäuser, Wetzlar, Germany), and high-resolution CCD Camera (JAI Corporation, Japan). The scanning system is driven by the software MetaCyte. The classifiers of the MetaCyte software allow the settings of image capture, exposure parameters, image processing, and cell processing steps. These classifiers contain variable criteria for cell selection taking into account cell characteristics like cell area, aspect ratio, concavity index, and signal intensity.

For capturing of cell images, a 40x Plan Neofluar air objective was used. Slide scanning procedure was started with the focus determination of cells in the DAPI channel in the selected scanning area. Then, a stack of five images within a distance $0.9\,\mu m$ were captured in the Cy3 and FITC channels. From each stack, a 2D image with all signals in focus was created and a local background reduction was performed applying two standard Top Hat filters. Overlapping or incomplete cell nuclei as well as nuclei with incorrect numbers of red and green signals were excluded from the analysis. For the analysis of fused or split signals, the distance of signals was measured in the XY positions as well as in Z positions. Between 100 and 870 cells were analyzed in the different samples. Each 2D image was displayed as gallery pictures presenting the cell number, the number of red and green signals, and the number of overlapping red and green signals. On the gallery screen also the results for each sample could be displayed as scatter diagram and/or as bar diagram. All data can be exported into common statistics and graphic software programs.

In parallel, every captured cell was analysed visually in order to compare visual and automated scoring of FISH signals. In contrast to automated scoring the visual analysis can be performed in two dimensions only.

2.5. Optimisation and Testing of Classifier Parameters. For optimization of the classifier parameters for RET/PTC rearrangements exhibiting split signals negative and positive control samples were analysed several times after changing the parameter settings for image capture, cell nucleus characteristics, and cell nucleus selection, by criteria such as nuclear area, aspect ratio, and concavity index of the nuclei, as well as size and distance of red and green signals. The final parameter settings for the automated analysis were optimised for the lowest numbers of false positive and false negative results.

2.6. Statistical Analysis. Frequencies of cells with split signals determined by automated analyses and by visual analyses were compared with an χ^2 test. Significant differences were accepted for P values less than .05 after adjustment for false detection by the Bonferroni method [12].

3. Results

21 PTCs were analyzed for chromosomal aberrations, and 22 PTCs were investigated for RET/PTC rearrangements. The RET/PTC status was determined by FISH analysis on interphase cells from the same primary cultures that were used for SKY analysis of chromosomal aberrations. For an evaluation of RET/PTC rearrangements an automated scoring system (Metafer4) was used and data were compared to FISH signals that had been scored visually.

3.1. SKY Analysis Detected Clonal Chromosome Rearrangements and Numerical Aberrations. SKY analysis revealed clonal chromosomal rearrangements in five out of 21 cases (24%). In two cases (10%) structural aberrations involving chromosome 11 could be observed. Additionally, numerical

chromosome aberrations could be detected in 13 cases (62%) with frequent losses of chromosomes 21 (six cases, 29%), 20 (five cases, 24%), 7, 10, and 22 (three cases each, 14%). Clonal chromosome aberrations are summarized in Table 1. Figure 1 shows an exemplary SKY image of case 402T exhibiting a deletion on chromosome 11 and i(11)(q10).

3.2. RET/PTC Rearrangements Are Present on FISH Analysis of Primary Cultures of PTC. FISH was carried out on interphase cell preparations from primary cultures of 22 PTCs using a combination of three YAC probes that were labelled in two different colours [7]. Cell nuclei exhibiting a rearranged RET gene show a split FISH signal in red and green in addition to an overlapping FISH signal, whereas normal cells show two overlapping FISH signals (Figure 2). Sixteen out of 22 PTCs (72%) exhibited RET rearrangements diagnosed by FISH interphase analysis (Table 1). The highest frequency of rearranged cells after FISH interphase analysis was 41% (case S430T). These 16 cases showed a significantly elevated frequency of split FISH signals compared to RPE cell line and S414 normal tissue which represent negative controls without any RET/PTC rearrangement. The frequency of false positive FISH signals in these control cells is in the order of 1–3% (Table 1). Therefore, we used a threshold of 7.1% of cells with a split FISH signal in order to define a RET/PTC-positive tumour as published earlier in [7]. The positive control cell line TPC1 showed 98% rearranged cells.

3.3. Comparison of Automated Scoring and Visual Scoring of Rearranged FISH Signals. In order to create the initial parameter settings for classifiers of the automated Metafer4 scoring system the RPE (human Retina pigment epithelial) cell line and primary culture of normal tissue from case S414, both with a normal karyotype, were used as negative control. The TPC1 cell line that was derived from a human papillary carcinoma carrying a RET/PTC1 rearrangement was used as a positive control. Based on these control cells the classifiers of the Metafer4 system were optimized several times by changing the parameter settings for cell nucleus characteristics and cell nucleus selection by criteria such as nuclear area, aspect ratio, and concavity index of the nuclei. For the scoring of fused and split FISH signals an optimisation of the parameters for minimum signal area, maximum distance of red and green signals, and the minimum signal intensity has been performed in multiple training procedures. The optimised parameters and their variability are given in Table 2. For testing the final parameter settings of the classifier the above-mentioned 22 PTCs were analysed using the automated scoring system as well as visual scoring of the recorded images. Results of both scoring procedures are shown in Table 1. The negative control cell lines showed a frequency of false positive RET/PTC rearrangement of 1–3%. The frequencies of RET/PTC positive cells among the PTC primary cultures varied between 1.0% and 41.5%. Concordance of results from automated and visual scoring was tested statistically. Statistical correlation analysis using the χ^2 test confirmed a concordance of the data from automated and visual analysis in 19 cases (86%). Only in three cases (S407T, S418T, and S422T) the automated

FIGURE 1: SKY analysis of case S402T showing a karyotype of 46, *XY*, del(11p), i(11q) (arrows). Isochromosome 11 is a clonal aberration in this case. The coloured chromosomes represent the false colour from the original RGB pictures of the multicolour FISH. Chromosomes were counterstained with DAPI (similar to Giemsa-banding).

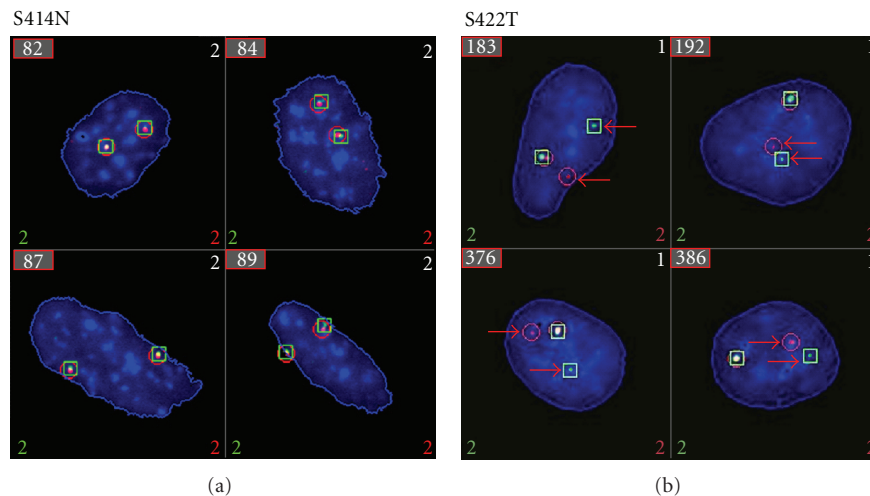(a)   (b)

FIGURE 2: FISH analysis of RET/PTC rearrangement: S414N nontumour cells showing two fused red and green signals; S422T tumour cells have one fused and one split red/green signal pair, indicating a RET gene rearrangement. Cells were hybridized with YAC probes 313F4 and 214H10 (FITC labelled, green signals) and 344H4 (Cy3 labeled, red signals). Arrows indicate the split signals of RET/PTC rearrangements.

and visual analysis differed significantly ($P < .05$; Bonferroni value, Figure 3).

4. Discussion

In this study, we describe karyotype abnormalities and rearrangements of the RET proto-oncogene in PTC from patients that were exposed to the radioiodine fallout of the Chernobyl accident. There is evidence from several studies that exposure to ionising radiation leads to the induction of chromosomal rearrangements that may result in gene alterations and deregulated gene expression [13, 14]. In PTC chromosomal breakpoints on 1p32-36, 1p11-13, 3p25-26, and 7q32-36 have previously been reported after conventional karyotyping [15]. Other cytogenetic studies on PTC showed a deletion on chromosome 11q [16] and a chromosome 2 rearrangement with an assumed tyrosine kinase gene at the breakpoint [17]. In addition, novel

breakpoints of structural rearrangements of chromosomes 4q, 5q, 6p, 12q, 13q, and 14q and of complex rearrangements have been reported using a complementary analysis of conventional karyotyping, SKY and FISH with BAC clones [8, 18, 19]. In our study, also rearrangements involving chromosome 11 could be detected in two cases (Table 1, Figure 1), indicating an important gene on this chromosome that might be involved in thyroid carcinogenesis. Besides the structural rearrangements it is remarkable that many numerical aberrations were observed mostly involving chromosomes 20, 21, and 22. Loss of chromosome 22 has already been reported to represent a cytogenetic marker for poor prognosis in thyroid cancer [20–22]. Thus, this observation in PTC may explain to some extent the more aggressive phenotypes of tumours that have developed after the Chernobyl accident.

Another frequent cytogenetic finding in PTC is the rearrangements of chromosome 10q with breakpoints at

TABLE 1: Karyotypes and RET/PTC rearrangements in papillary thyroid carcinomas from Ukraine.

Case	Age/gender	SKY analysis Clonal aberrations[#]	RET/PTC rearrangement (rearranged cells %)		
			No. of cells scored	Automated scoring with Metafer4	Visual scoring of Metafer4 recorded cells
RPE (control w/o RET/PTC)	—/f	—	186	0.7	1.1
TPC1 (control with RET/PTC)	—/f	der(1)t(1;3), der(1)t(1;21), del(3p), i(8p), der(10)t(10q;3p), der(10)t(10q;1q); del(10p), −21	103	98.1	97.1
S414N (control w/o RET/PTC)	33/f	n.a.	180	3.1	1.1
S399T	13/m	—	103	17.7[+]	8.7[+]
S400T	19/m	−7, −12, −21, −20	354	13.3[+]	16.1[+]
S402T	34/m	−19, −11, i(11)(q10)	139	12.1[+]	10.8[+]
S403T	12/m	del(11p)	n.a.		
S404T	16/f	−11, −20, −21, −22	154	11.6[+]	11.7[+]
S405T	16/f	−10, −12	233	19.4[+]	21.0[+]
S407T	19/f	−10, −16, −18, −20, −21	608	5.4[*]	10.7[*+]
S408T	25/m	−2, −5, −7, −10,−13, −17, −18, −22	715	2.1	1.5
S409T	28/f	n.a.	122	10.6[+]	13.9[+]
S411T	12/f	—	793	2.2	2.0
S412T	21/f	−7, −8, −21	267	12.9[+]	9.0[+]
S413T	18/f	−14, −21	220	5.2	5.9[+]
S414T	33/f	−20	67	23.8[+]	20.9[+]
S416T	15/m	—	211	1.0	2.4
S418T	27/m	−16	262	12.9[*+]	3.1[*]
S420T	28/f	—	190	14.2[+]	9.5[+]
S422T	31/m	—	756	23.2[*+]	14.6[*+]
S428T	21/m	—	683	11.0[+]	16.8[+]
S429T	13/f	−9, −22	330	20.6[+]	16.7[+]
S430T	32/f	—	102	41.5[+]	33.3[+]
S431T	21/f	−9, −19, −20	110	33.8[+]	30.0[+]
S432T	26/m	n.a.	80	12.2[+]	12.5[+]
S437T	22/f	−21	126	15.1[+]	13.5[+]

[#] At least 15 metaphases were analysed by SKY.
—: normal karyotype.
n.a.: not analysed.
[*] Significant difference between automated and visual scoring (χ^2 test, $P < .05$; Bonferroni value).
[+] Significant difference to respective negative control (S414N; Fisher's exact test, $P < .05$).

10q11.2 that lead to an activation of the RET proto-oncogene [23, 24]. The most frequent rearrangements are paracentric inversions on chromosome 10q leading to the oncogenes RET/PTC1 and RET/PTC3. Thus, these chromosomal rearrangements lead to transcribed fusion genes that affect the MAPkinase pathway. Investigations of these RET/PTC rearrangements are important in PTC since they represent frequent alterations and molecular targets for therapeutic interventions [25, 26]. In this study, we have investigated RET/PTC rearrangements in the PTC using an interphase FISH approach that allows to detect RET rearrangements regardless of the specific fusion partner involved at a single-cell level [7]. The frequency of RET/PTC-positive cases of 72% is in line with earlier reports on tissue sections using a three-dimensional evaluation of FISH signals either with laser-scanning microscopy or Apotome-equipped fluorescence microscopy [7, 27]. The reported genetic heterogeneity could be confirmed in this study since only a subpopulation of tumour cells showed the RET/PTC rearrangement.

Although interphase FISH analysis has a number of advantages in detecting gene rearrangements, it is a challenge to score adequately the frequency of rearranged cells.
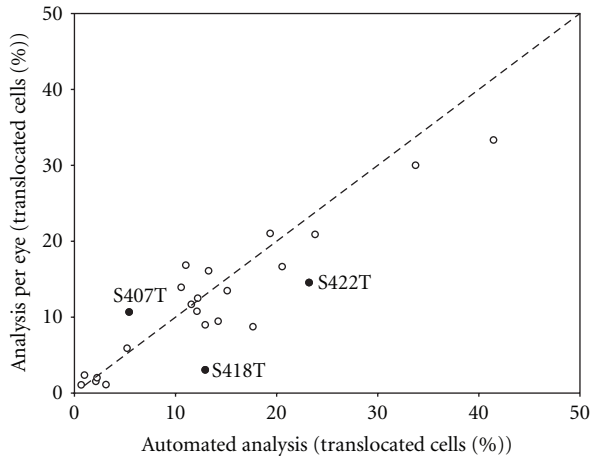
FIGURE 3: Correlation analysis using the χ^2 test. For three samples the data differed significantly ($P < .05$; Bonferroni P value) between automatic and visual analysis (filled symbols).

TABLE 2: Classifier parameters for cell and signal selection.

Parameters	Variability of parameters	Finally optimized parameters
Cell selection parameters		
Minimum cell nucleus area	0 to 32,000 μm^2	120 μm^2
Maximum cell nucleus area	0 to 32,000 μm^2	500 μm^2
Maximum concavity depth	0 to 1	0.35
Maximum aspect ratio	1 to 10	2.5
Signal parameters		
Min. absolute signal area	0 to 100 μm^2	0.1 μm^2
Max. distance of fused signals	0.1 to 100 μm	0.8 μm
Min. of max. signal intensity	0 to 100%	33%

A major problem that also affects the sensitivity of the FISH approach is the inevitable scoring of false positive FISH signals due to random generation of rearrangement-positive FISH signals. The choice of adequate FISH probes (fusion probes or split probes for the detection of a rearranged cell) is one issue that has to be addressed; an impartial evaluation of FISH signals is another important issue. In this study, we have compared visual inspection of FISH signals with an automated evaluation. In the automated process, a correct detection of FISH signals is a great challenge, since FISH signals exhibit large variations in shape, size, and intensity [28]. After cell nucleus selection and correct FISH signal detection, a discrimination of nuclei with and without RET/PTC rearrangement could be achieved by measuring the signal distances and defining the minimal distance to diagnose a split FISH signal. Therefore, cells with 100% RET/PTC-positive signals were needed. TPC1 cell line has this feature and showed in our study 97% and 98% positivity, respectively. The automated analysis reported in this study was optimised to detect RET/PTC rearrangements by means of a YAC probe set covering the RET gene locus. Differential labelling of the YAC probes in red and green resulted in overlapping red/green signals for the wild-type RET gene and in a split red and green FISH signals for the rearrangement. The automated evaluation of FISH signals revealed matching results in 87% of the 22 cases with the visual analysis of FISH signals. A possible explanation for three misclassified cases is a bias of the investigator scoring visually towards RET/PTC-positive or -negative cells, especially in cases with high background signals. Also different cell features in those three cases may account for the observed discrepancy. An additional difference in fusion counting automatically or by eye is that the automated system is measuring the distance 3-dimensionally, whereas directly at the microscope or with captured images a visual scoring is performed at 2D projection. A comparison of automated and manual evaluation of interphase FISH results was only presented by Kajtár et al [29] in case of BCR/ABL rearrangements in CML patients. Although the probe design is different (fusion probe versus split signal probe), we received a similar good concordance of automated and manual evaluation results. We have demonstrated here for the first time the usage of the 3D automated FISH analysis for the detection of RET/PTC rearrangements in PTC.

In conclusion, we have shown that chromosomal rearrangements (5 out of 21) and rearrangements of the RET gene (16 out of 22) are frequent in papillary thyroid carcinomas from patients of the Ukraine after the Chernobyl accident. For the detection of RET/PTC rearrangements we have demonstrated an automated FISH analysis approach which provides reliable results in higher cell numbers. The results of RET/PTC rearrangements again indicate a genetic heterogeneity since only subpopulations of tumour cells carried the RET/PTC rearrangement.

Acknowledgments

References

[1] D. Perrotti, C. Jamieson, J. Goldman, and T. Skorski, "Chronic myeloid leukemia: mechanisms of blastic transformation," *Journal of Clinical Investigation*, vol. 120, no. 7, pp. 2254–2264, 2010.

[2] H. Zitzelsberger, V. Bauer, G. Thomas, and K. Unger, "Molecular rearrangements in papillary thyroid carcinomas," *Clinica Chimica Acta*, vol. 411, no. 5-6, pp. 301–308, 2010.

[3] J. D. Rowley, "Identification of a translocation with quinacrine fluorescence in a patient with acute leukemia," *Annales de Genetique*, vol. 16, no. 2, pp. 109–112, 1973.

[4] D. Pinkel, T. Straume, and J. W. Gray, "Cytogenetic analysis using quantitative, high-sensitivity, fluorescence hybridization," *Proceedings of the National Academy of Sciences of the United States of America*, vol. 83, no. 9, pp. 2934–2938, 1986.

[5] E. Schröck, S. Du Manoir, T. Veldman et al., "Multicolor spectral karyotyping of human chromosomes," *Science*, vol. 273, no. 5274, pp. 494–497, 1996.

[6] T. Veldman, C. Vignon, E. Schröck, J. D. Rowley, and T. Ried, "Hidden chromosome abnormalities in haematological malignancies detected by multicolour spectral karyotyping," *Nature Genetics*, vol. 15, no. 4, pp. 406–410, 1997.

[7] K. Unger, H. Zitzelsberger, G. Salvatore et al., "Heterogeneity in the distribution of RET/PTC rearrangements within individual post-chernobyl papillary thyroid carcinomas," *The Journal of Clinical Endocrinology and Metabolism*, vol. 89, no. 9, pp. 4272–4279, 2004.

[8] H. Zitzelsberger, L. Lehmann, L. Hieber et al., "Cytogenetic changes in radiation-induced tumors of the thyroid," *Cancer Research*, vol. 59, no. 1, pp. 135–140, 1999.

[9] S. M. Jhiang, D. R. Caruso, E. Gilmore et al., "Detection of the PTC/ret(TPC) oncogene in human thyroid cancers," *Oncogene*, vol. 7, no. 7, pp. 1331–1337, 1992.

[10] Y. Ishizaka, F. Itoh, T. Tahira et al., "Presence of aberrant transcripts of ret proto-oncogene in a human papillary thyroid carcinoma cell line," *Japanese Journal of Cancer Research*, vol. 80, no. 12, pp. 1149–1152, 1989.

[11] A. Riches, C. Peddie, S. Rendell et al., "Neoplastic transformation and cytogenetic changes after gamma irradiation of human epithelial cells expressing telomerase," *Radiation Research*, vol. 155, no. 1, part 2, pp. 222–229, 2001.

[12] C. E. Bonferroni, "Teoria statistica delle classi e calcolo della probabilità," *Pubblicazioni del R Istituto Superiore di Scienze Economiche e Commerciali di Firenze*, vol. 8, pp. 3–62, 1936.

[13] H. B. Forrester and I. R. Radford, "Ionizing radiation-induced chromosomal rearrangements occur in transcriptionally active regions of the genome," *International Journal of Radiation Biology*, vol. 80, no. 10, pp. 757–767, 2004.

[14] K. Unger, J. Wienberg, A. Riches et al., "Novel gene rearrangements in transformed breast cells identified by high-resolution breakpoint analysis of chromosomal aberrations," *Endocrine-Related Cancer*, vol. 17, no. 1, pp. 87–98, 2010.

[15] L. Roque, V. M. Nunes, C. Ribeiro, C. Martins, and J. Soares, "Karyotypic characterization of papillary thyroid carcinomas," *Cancer*, vol. 92, no. 10, pp. 2529–2538, 2001.

[16] E. Olah, E. Balogh, F. Bojan, F. Juhasz, V. Stenszky, and N. R. Farid, "Cytogenetic analyses of three papillary carcinomas and a follicular adenoma of the thyroid," *Cancer Genetics and Cytogenetics*, vol. 44, no. 1, pp. 119–129, 1990.

[17] L. Lehmann, K. M. Greulich, H. Zitzelsberger et al., "Cytogenetic and molecular genetic characterization of a chromosome 2 rearrangement in a case of human papillary thyroid carcinoma with radiation history," *Cancer Genetics and Cytogenetics*, vol. 96, no. 1, pp. 30–36, 1997.

[18] H. U. G. Weier, T. B. Tuton, Y. Ito et al., "Molecular cytogenetic characterization of chromosome 9-derived material in a human thyroid cancer cell line," *Cytogenetic and Genome Research*, vol. 114, no. 3-4, pp. 284–291, 2006.

[19] C. M. Lu, J. Kwan, A. Baumgartner et al., "DNA probe pooling for rapid delineation of chromosomal breakpoints," *Journal of Histochemistry and Cytochemistry*, vol. 57, no. 6, pp. 587–597, 2009.

[20] S. Hemmer, V. M. Wasenius, S. Knuutila, K. Franssila, and H. Joensuu, "DNA copy number changes in thyroid carcinoma," *American Journal of Pathology*, vol. 154, no. 5, pp. 1539–1547, 1999.

[21] B. Singh, D. Lim, J. C. Cigudosa et al., "Screening for genetic aberrations in papillary thyroid cancer by using comparative genomic hybridization," *Surgery*, vol. 128, no. 6, pp. 888–894, 2000.

[22] B. Perissel, I. Coupier, M. De Latour et al., "Structural and numerical aberrations of chromosome 22 in a case of follicular variant of papillary thyroid carcinoma revealed by conventional and molecular cytogenetics," *Cancer Genetics and Cytogenetics*, vol. 121, no. 1, pp. 33–37, 2000.

[23] M. Santoro, F. Carlomagno, I. D. Hay et al., "Ret oncogene activation in human thyroid neoplasms is restricted to the papillary cancer subtype," *Journal of Clinical Investigation*, vol. 89, no. 5, pp. 1517–1522, 1992.

[24] M. A. Pierotti, M. Santoro, R. B. Jenkins et al., "Characterization of an inversion on the long arm of chromosome 10 juxtaposing D10S170 and RET and creating the oncogenic sequence RET/PTC," *Proceedings of the National Academy of Sciences of the United States of America*, vol. 89, no. 5, pp. 1616–1620, 1992.

[25] C. Lanzi, G. Cassinelli, V. Nicolini, and F. Zunino, "Targeting RET for thyroid cancer therapy," *Biochemical Pharmacology*, vol. 77, no. 3, pp. 297–309, 2009.

[26] Y. E. Nikiforov, "Thyroid carcinoma: molecular pathways and therapeutic targets," *Modern Pathology*, vol. 21, supplement 2, pp. S37–S43, 2008.

[27] K. Unger, L. Zurnadzhy, A. Walch et al., "RET rearrangements in post-Chernobyl papillary thyroid carcinomas with a short latency analysed by interphase FISH," *British Journal of Cancer*, vol. 94, no. 10, pp. 1472–1477, 2006.

[28] K. Truong, J. Boenders, Z. Maciorowski et al., "Signal amplification of FISH for automated detection using image cytometry," *Analytical Cellular Pathology*, vol. 13, no. 3, pp. 137–146, 1997.

[29] B. Kajtár, G. Méhes, T. Lörch et al., "Automated fluorescent in situ hybridization (FISH) analysis of t(9;22)(q34;q11) in interphase nuclei," *Cytometry Part A*, vol. 69, no. 6, pp. 506–514, 2006.

The Scientific
World Journal

Gastroenterology
Research and Practice

MEDIATORS
of
INFLAMMATION

Journal of
Diabetes Research

Disease Markers

Journal of
Immunology Research

International Journal of
Endocrinology

PPAR Research

BioMed
Research International

Hindawi

Submit your manuscripts at
http://www.hindawi.com

Journal of
Ophthalmology

Stem Cells
International

eCAM

Evidence-Based
Complementary and
Alternative Medicine

Journal of
Obesity

Journal of
Oncology

Computational and
Mathematical Methods
in Medicine

Behavioural
Neurology

Parkinson's
Disease

AIDS
Research and Treatment

Oxidative Medicine and
Cellular Longevity